

Analysis of a novel soft switching bidirectional DC-DC converter for electric vehicle

Podila Purna Chandra Rao¹, Radhakrishnan Anandhakumar¹, L. Shanmukha Rao²

¹Department of Electrical Engineering, Faculty of Engineering and Technology, Annamalai University, Chidambaram, India

²Department of Electrical and Electronics Engineering, Kallam Haranadhareddy Institute of Technology, Dasaripalem, India

Article Info

Article history:

Received Aug 2, 2022

Revised Sep 30, 2022

Accepted Jan 11, 2023

Keywords:

DC-DC converter

High gain

MPPT

Pulse width modulation

Solar PV system

Zeta converter

ABSTRACT

A bidirectional converter (BDC) designed with high voltage gain and it is incorporated with the soft-switching operations to the insulated gate bipolar transistors (IGBTs). The main dual operating characteristics of this converter are boost and buck modes respectively. In order to achieve the reduced switching losses and improved efficiency, the main IGBTs are operated at zero-current (ZC) while the IGBTs commutating from turn-on to turn-off state. The ZC turn-off operation is obtained with the aid of soft-switched cell, which consists of resonant inductor (L_r), capacitor and additional IGBTs. In this work, the design simulation analysis for high-gain BDC was performed by 70/300 V power system with the maximum 800 W output power under the operating frequency of 50 kHz. The efficiency for the high-gain soft-switched BDC was obtained as 96.5% when it is operating in boost mode and efficiency of 97% was achieved for the buck mode operation. The simulation evaluations of the above said converters were performed by using MATLAB/Simulink.

This is an open access article under the [CC BY-SA](https://creativecommons.org/licenses/by-sa/4.0/) license.



Corresponding Author:

Podila Purna Chandra Rao

Department of Electrical Engineering, Faculty of Engineering and Technology, Annamalai University

Annamalai Nagar, Chidambaram, Tamil Nadu 608001, India

Email: purnachandrarao.phd@gmail.com

1. INTRODUCTION

These days, power converters are in high demand due to their widespread use in emergency power sources like fuel cells and super capacitors. Getting electricity from low to high voltage and back again is a vital function of isolated bidirectional DC-DC converters in battery backup systems. To compensate for the wide variation in source voltage (67.5 to 35%), a transformer-less DC-DC converter [1] with a high voltage gain of up to 3 kV is constructed by cascading switches and capacitors (19 arrays in all) and operating them in hard-switching mode. Diode-capacitor circuits are one method that has been employed by several researchers to achieve high gain [2], [3]. Inverted dual converters [4] that transmit power in both ways may boost high voltage gain converter performance. SCRs switch output power between channels using semiconductor converters.

Recent studies have used isolated full-bridge DC-DC converters with large voltage gains for high-efficiency battery storage [5]. Push-pull [6] and half bridge [7] current-fed isolated converters are hard-switching. Subsequently, snubber capacitors, transformer leakage inductances, and current-fed high voltage gain resonant full bridge converters were used to achieve zero voltage switching [8]. Passive and active lossless snubbers provide zero-voltage switching (ZVS) at semiconductor switches in certain current-fed isolated half-bridge converters [9]. This architecture performed zero current switched (ZCS) turn-off and ZVSturn on operations using active clamp circuits [10] and separated converters [11].

A hard-switching multiphase high gain, high power, non-isolated step-up converter with more phases reduces input current ripple [12]–[14].

Subsequent studies concentrated on developing small, cost-effective, and non-isolated converters for use in battery backup systems. A passive resonant circuit was added to the design of non-isolated, high-voltage-gain boost converters [15]–[18] to enable soft switching operations at the converter's switching devices and diodes. They achieved soft-commutation zero voltage transition (ZVT) in the MOSFETs and diodes by keeping the resonance frequency below their operating frequency. The team then focused on building non-isolated bidirectional DC-DC converters [19] for use in electric vehicles' secondary power supply systems; these converters use simple series resonant components to provide ZVS turn-on of their main switching devices. Non-isolated high gain boost converters [20] were constructed by using a parallel resonant circuit inductor capacitor capacitor (LCC) and an additional voltage multipliers cell. They were able to activate the diodes and primary switches using zero voltage (ZV) action and zero current (ZC) action, respectively. Although low efficiency was obtained with very low power and very high switching frequency (150 kHz). However, a unidirectional current fed converter [21], [22] was created without the usage of voltage multiplier cells; it reached 95.5% efficiency at working frequencies larger than 100 kHz and had ZC turn-off operations for its switches. According to Zhang and Chau [17], several non-isolated type converter topologies may be employed in soft-switching scenarios. To use electromechanical braking systems in battery-powered vehicles, researchers at MIT devised a passive lossless bidirectional converter (BDC) [23] that required no voltage for operation. Minimal efforts are made to reduce the input voltage (V_{in}), input power, and switching frequency [24]. However, it has reached a maximum efficiency of roughly 94% when used with very low output power levels.

Based on past high gain BDC designs, hard and soft-switching variants are examined to reduce switching losses, boost output power, switching frequency, and efficiency. A non-isolated bidirectional DC-DC converter under ZC switching commutations has been proposed and constructed. This chapter shows a high-gain non-isolated bidirectional DC-DC converter using active and passive resonant circuits. The present study sought to minimise switching losses during soft-switching switches [25].

As seen in Figure 1, the overall structure of the auxiliary power supply systems employed by electric cars is shown. In general, while the BDC is operating in boost mode, the output voltage (V_o) is four times greater than the applied V_{in} . A fully charged battery is used to supply power to the source voltage while operating in the boost mode of operation. In electric vehicles, the V_o generated in boost mode is sent into an isolated full bridge converter, which drives the auxiliary systems with the power generated. Instead of operating in buck mode, the converter may be used to charge the battery, which is connected in series with the converter.

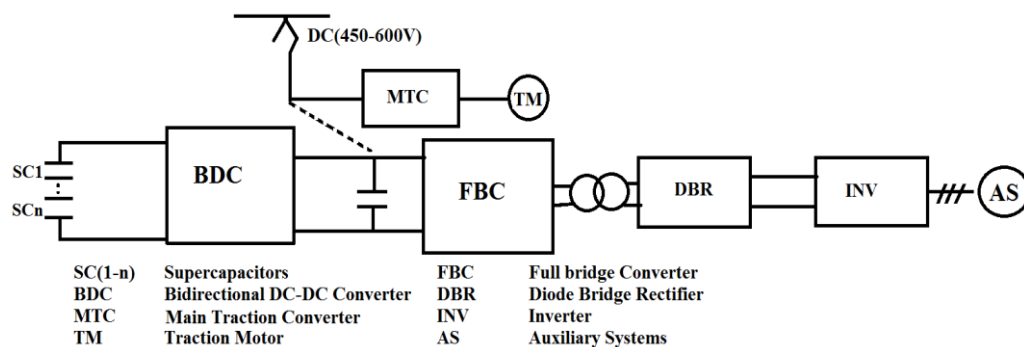


Figure 1. Electric cars' auxiliary batteries are used in case of a power outage

2. PROPOSED CONVERTER DESCRIPTION

Figure 2 depicts a schematic representation of the proposed converter. An voltage gain and it is incorporated with the soft-switching operations to the insulated gate bipolar transistors (IGBT) (S1-6), two input inductors (L_1 , L_2), an auxiliary inductor (L_r), and a capacitor make up the majority of the circuit's components (C_r). The proposed circuit consists of two main switches, S1 and S2, which operate in boost mode, and main switches, S3, and S4, which operate in buck mode. In all modes of operation, the auxiliary switches S_p and S_q , as well as the resonant inductor (L_r) and C_r , are components of the auxiliary resonant cell, which is responsible for achieving ZCS turn-off in both modes of operation. When in boost mode of operation, the S1, S2 are always switched on, while the S3, S4 are always turned off. In order to achieve ZCS

functioning, the auxiliary switches S5, S6 are switched on for a brief period of time before the main switches are shut off. Additionally, when operating in buck mode, the S1, S2 are both switched off during the operation process. This mode is activated by switching on the primary switches S3, S4. On the basis of the essential waveforms displayed in Figure 3, the functioning of the proposed converter in boost and buck modes is explained, and its corresponding circuits with the direction of current flow are illustrated in Figure 4.

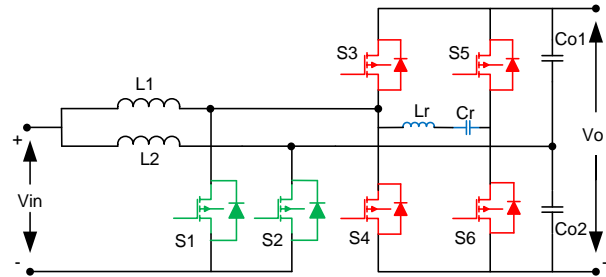


Figure 2. High gain bidirectional ZCS DC-DC converter proposed

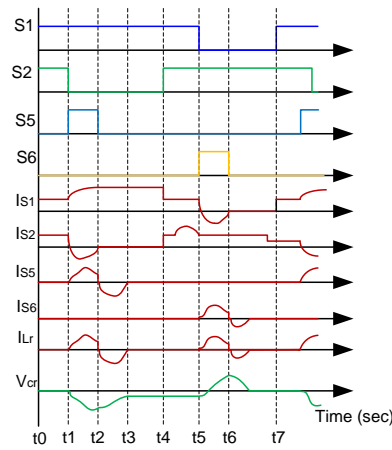


Figure 3. Theoretical waveforms: boost mode

3. PRINCIPLE OF OPERATION OF PROPOSED CONVERTER

3.1. Boost mode

First interval (t_0 - t_1): main IGBT S1 is activated at time t_0 . As the input inductor's current increases, so does the current flowing through IGBT S1. The IGBT's S2 is in its conduction state before $t=0$ (t_0). For the first stage, the resonant tank current must go via the IGBT S1 to cancel out the resonance between L_r and C_r . To illustrate the IGBT's S1, current (i_{s1}), consider (1):

$$I_{s1} = \frac{V_1}{L_r} (t - t_0) - \frac{V_1}{Z} \cos \omega (t - t_0) + I_0 \quad (1)$$

Second interval (t_1 - t_2): to accomplish S2's ZC turn-off at time t_1 , auxiliary IGBT S5 is activated as shown in Figure 4(a). The secondary IGBT S5 is switched off once again at time t_2 . When the input inductor L2 is disconnected from the power source, the energy stored there is released and sent to the load. t_2 Input current I_o at the device's output is identical to the current via IGBT S1. At time t_2 , a second S2 anti-parallel IGBT diode is conducting. The following equation describes the relationship between the voltage and current across the auxiliary capacitor C_r (S2,S5):

$$I_{s2} = I_0 - \frac{V_1}{Z} (t - t_2) \cos \omega (t - t_2) \quad (2)$$

$$V_{Cq} = -V_1 \cos \omega (t - t_1) \quad (3)$$

Third interval (t_2 - t_3): since IGBT S1 has been conducting current since t_0 , when S2 is shut off at time t_2 , a negative current flows through IGBT S5, turning on its anti-parallel diode. It is the job of L2-C2-R

to deliver the energy stored in inductor L2 to the load. The IGBT S5's anti-parallel diode is disabled after this period has elapsed. The equivalent circuit is shown in Figure 4(b).

Fourth interval (t3-t4): this interval is comprised of the IGBT S1 remaining in conduction for a short duration of time and then the input inductor L1 accumulating the energy during the turn-on phase of the IGBT S1 for a longer period of time. The equivalent circuit is shown in Figure 4(c). Fifth interval (t4-t5): this interval is analogous to the t0-t1 period in that the IGBT S1 stays in conduction save for the gating signals applied to S2 during this interval.

Sixth interval (t5-t6): the auxiliary IGBT S6 is switched on at t5 in order to obtain the turn-off at ZC for S1, while at the same time, the IGBT S1 current gradually decreases to zero and then reverses direction after that. The resonating interval is the time interval during which the resonating frequency is heard. The equivalent circuit is shown in Figure 4(d). The gentle turn-off is achieved by the application of the resonant tank current created by Lr, Cr. The following are the definitions for the voltage and current expressions:

$$I_{LP} = -\frac{V_{cq}}{\sqrt{L_p/C_p}} \sin \omega(t - t_5) \quad (4)$$

$$V_{cq} = V_1 \cos \omega(t - t_5) + I_0 \quad (5)$$

The seventh interval (t6-t7) corresponds to the same time period as the period from t2-t4. The equivalent circuit is shown in Figure 4(e).

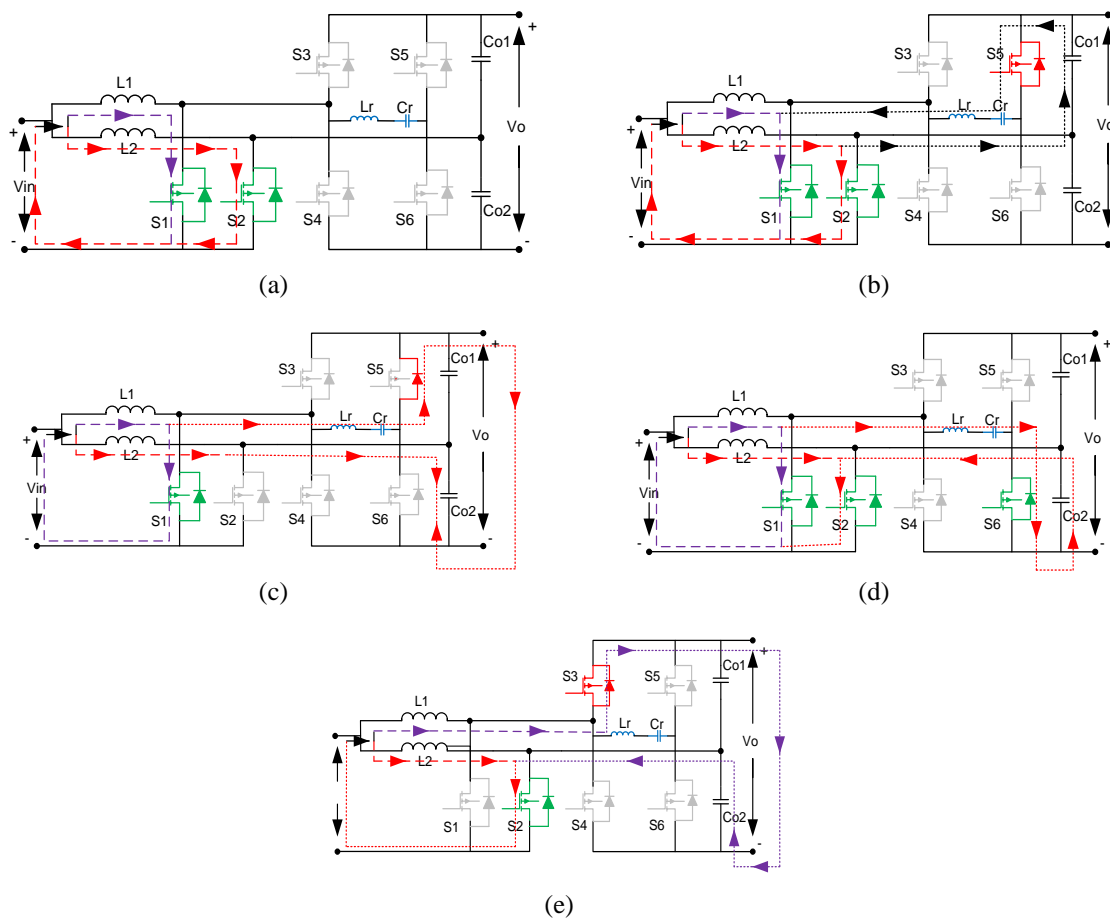


Figure 4. Functioning of the proposed converter in boost mode and its corresponding circuits with the direction of current flow: (a) current flow equivalent circuits of each interval -boost mode during interval t0-t1 and t4-t5, (b) current flow equivalent circuits of each interval -boost mode during interval t1-t2, (c) current flow equivalent circuits of each interval -boost mode during interval t3-t4, (d) current flow equivalent circuits of each interval -boost mode during interval t5-t6, and (e) current flow equivalent circuits of each interval-boost mode during interval t6-t7

4. DESIGN ANALYSIS

The suggested converter design analysis is outlined here. Designing an additional series resonant circuit was suggested for this converter in order to accomplish ZC turn-off of the semiconductor switching devices. It was accomplished in either direction of the converter's power flow. In both the boost and buck modes, the current through the IGBTs S1-4 grows when the transistors are switched on because of the resonant tank current. Peak resonant tank current via the IGBTs informed our choice of Cr values (S1-S2). Increasing the value of the Cr will cause the peak current to decrease via the IGBTs S1,S2, and decreasing the value of the Cr will have the opposite effect. The soft-turn-off length, or total time of resonance, may go up or down, depending on the values of the Cr, which can be positive or negative. The likelihood of the IGBTs shutting off at ZC increases as Lr resonant inductance values increase (S1-4). In (6) provides an approach that may be used to estimate the DC voltage conversion ratio:

$$\frac{V_o}{V_{in}} = \frac{1}{2\pi} \frac{f}{f_r} \left(\frac{k}{2} + \frac{1}{k} - \sqrt{\frac{1}{k^2} - 1} + 2\pi - \sin^{-1} k \right) + \frac{\delta t}{T} \quad (6)$$

where f is switching frequency; fr is resonant frequency; Vo is output voltage; Vin is input voltage; k is constant; $\frac{\delta t}{T}$ -duty cycle:

$$\frac{V_o}{V_{in}} = \frac{1}{2\pi} \frac{f}{f_r} (2\pi) + \frac{\delta t}{T} \quad (7)$$

$\frac{f}{f_r}$ is a fixed value, and change the Vo by changing the the $\frac{\delta t}{T}$ and the maximum is given by:

$$\left(\frac{\delta t}{T} \right) \frac{V_o}{V_{in}} \frac{f}{f_{r_{max}}} \quad (8)$$

$$f_r = \frac{1}{2\pi\sqrt{L_q C_q}} \quad (9)$$

The ZC turn-off condition for S1-4 can be obtained if as (10) when the parameter (k) is less than one ($k < 1$).

$$k = \frac{I_m}{V_{in}} \sqrt{\frac{L_q}{C_q}} \leq 1 \quad (10)$$

Where k- is constant ($k \leq 1$). Selection of input inductor the as (11) was used to find the value of input inductor:

$$L_1 = L_2 = \frac{D_1 * V_1}{f_{sw} * \Delta I} \quad (11)$$

Consideration of some allowance for input inductors value is chosen as 200 μ H 3.3.2 selection of output capacitor (Co) as (12) was used to find the value of Co:

$$C_{01} = C_{02} = \frac{I_o * dc * (1-dc) * 1000}{f_{sw} * V_{p(max)}} \quad (12)$$

Consideration of some allowance for Co value is chosen as 470 μ F.

5. SIMULATION ANALYSIS

As a first step, the proposed soft-switching operations of the converter are simulated using MATLAB/Simulink, which takes into account the supplied source voltage of 70 V in boost mode and 300 V in buck mode. According to the equation, the working frequency of this converter is around 50 kHz, and the resonant circuit frequency is 0.159 MHz (13). Their primary IGBTs will have soft-switching if (10) is satisfied. Open-loop simulations were used to create and test this converter. As shown in the boost mode waveforms shown in Figure 5(a)-(e), the collector-emitter voltage and currents of the IGBTs (S1, S2), the current through the auxiliary inductor Lr, and the voltages across the auxiliary capacitors Cr, are all consistent with the IGBT S1 and auxiliary IGBTs Sp being turned off at ZC. The buck mode simulations were also run, and the resulting waveforms can be seen in Figures 6(a)-(d). According to Table 1, a 70/300 V prototype was built for validation of the converter design's simulation findings utilising the components and parameters listed. The boost and buck modes each had duty cycles of 66 and 45%, respectively.

- Efficiency comparison

The general function of output power to the input power is used to do efficiency analysis of this converter. When this converter operated at 400 W output power, the efficiency was obtained as 96.5% in boost mode at 70 V and 97% in buck mode at 300 V input voltage. At 500 W output power, this converter operated effectively with high gain. The efficiencies of both boost and buck modes under 800 W output power levels are shown in Figures 7 and 8, which are simulated and compared with the experimental result. The simulation efficiencies of the converter designs are 97.6 and 98.5% for the boost and buck modes, respectively.

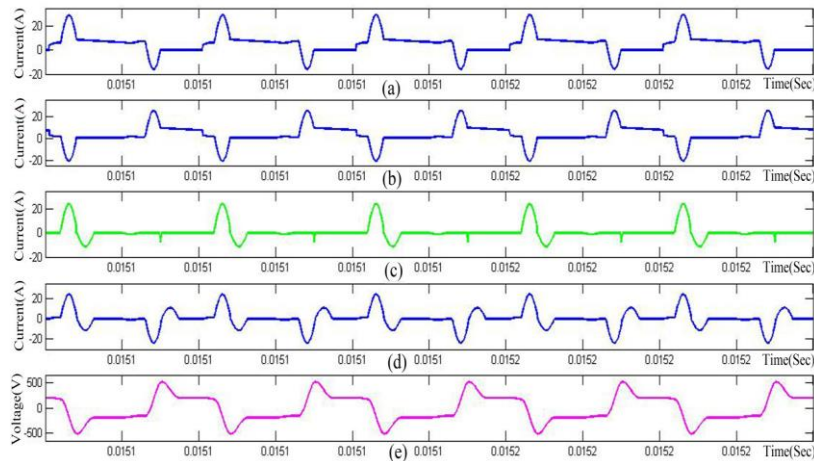


Figure 5. Boost mode operation waveforms: (a) IS1-switch current of S1, (b) IS2-switch current of S2, (c) IS5-auxiliary switch current of S5, (d) ILr-Lr current, and (e) VCr-Cr voltage: boost mode

Table 1. Parameters	
Parameter	Value
Vin	70 V
Vo	300 V
Inductance (L1, L2)	200 μ H
Lr	20 μ H
Cr	40 nF
Co	470 μ F
Switching frequency	50 kHz

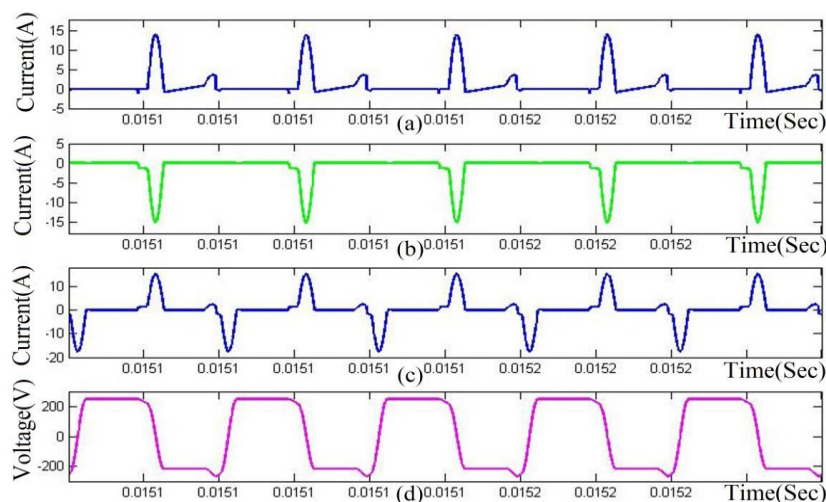


Figure 6. Buck mode operation waveforms: (a) IS3-switch current of S3, (b) IS5-auxiliary switch current of S5, (c) ILr-Lr current, and (d) VCr-Cr voltage: buck mode

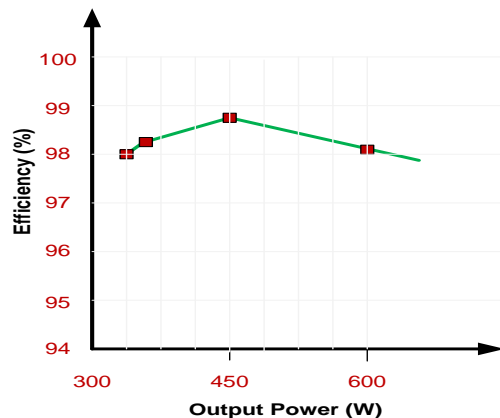


Figure 7. Measured and simulated efficiency curves for boost mode

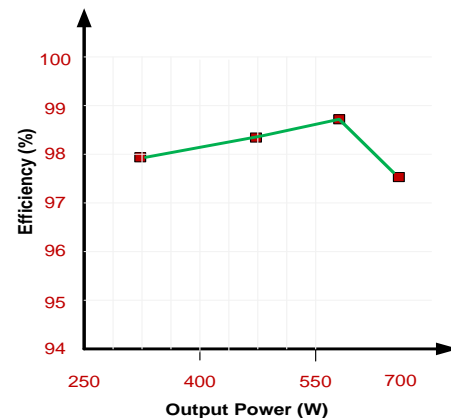


Figure 8. Measured and simulated efficiency curves for buck mode

6. CONCLUSION

In this research, a high-gain soft-switching BDC was designed with the express purpose of finding use in electric cars. The primary IGBTs were soft-switched off in both the boost (discharging) and buck (charging) modes with the assistance of the auxiliary IGBTs, auxiliary inductor, and auxiliary capacitors. During the boost mode, the capacitors were discharged, and during the buck mode, they were charged. Both boost and buck modes of operation on this converter's 500 and 800 W outputs have been tested and evaluated. IGBTs were turned off with ZC because of their minimal turn-off switching power losses. At 400 W of output power, efficiencies of 96.5 and 97% were achieved in boost and buck modes, respectively. This suggests that the suggested converter might be useful in any energy storage system for electric vehicles.





REFERENCES

- [1] D.-Y. Lee, M.-K. Lee, D.-S. Hyun, and I. Choy, "New zero-current-transition PWM DC/DC converters without current stress," *IEEE Transactions on Power Electronics*, vol. 18, no. 1, pp. 95–104, Jan. 2003, doi: 10.1109/TPEL.2002.807206.
- [2] L. Schuch, C. Rech, H. L. Hey, H. A. Grundling, H. Pinheiro, and J. R. Pinheiro, "Analysis and design of a new high-efficiency bidirectional integrated ZVT PWM converter for DC-bus and battery-bank interface," *IEEE Transactions on Industry Applications*, vol. 42, no. 5, pp. 1321–1332, Sep. 2006, doi: 10.1109/TIA.2006.880847.
- [3] S. J. Chiang, K. T. Chang, and C. Y. Yen, "Residential photovoltaic energy storage system," *IEEE Transactions on Industrial Electronics*, vol. 45, no. 3, pp. 385–394, Jun. 1998, doi: 10.1109/41.678996.
- [4] R. Redl, B. Molnar, and N. Sokal, "Class-E resonant regulated DC/DC power converters: analysis of operation, and experimental results at 1.5 MHz," in *1983 IEEE Power Electronics Specialists Conference*, Jun. 1983, pp. 50–60, doi: 10.1109/PESC.1983.7069839.
- [5] S. Mohan and E. P. Cheriyan, "Bilateral converter to interface small battery energy storage system with micro-grid," in *2012 IEEE Students' Conference on Electrical, Electronics and Computer Science*, Mar. 2012, pp. 1–4, doi: 10.1109/SCEECS.2012.6184785.
- [6] K.-H. Liu, R. Oruganti, and F. C. Y. Lee, "Quasi-resonant converters-topologies and characteristics," *IEEE Transactions on Power Electronics*, vol. 2, no. 1, pp. 62–71, Jan. 1987, doi: 10.1109/TPEL.1987.4766333.
- [7] C. M. Liaw, T. H. Chen, S. J. Chiang, C. M. Lee, and C. T. Wang, "Small battery energy storage system," in *IEE Proceedings B (Electric Power Applications)*, 1993, pp. 7–17, doi: 10.1049/ip-b.1993.0002.
- [8] E. Tatakis and N. Polyzos, "A novel approach to evaluate the behavioral characteristics of zero-voltage switching quasi-resonant converters," in *PESC Record. 27th Annual IEEE Power Electronics Specialists Conference*, 1996, pp. 1388–1393, doi: 10.1109/PESC.1996.548763.
- [9] K. K. Saravanan, S. Rajalakshmi, N. Stalin, and S. Titus, "New zero current transition PWM DC/DC converter without current stress," in *IEEE-International Conference on Advances in Engineering, Science and Management, ICAESM-2012*, 2012, pp. 566–570, doi: 10.1109/pesc.2001.954261.
- [10] M. Srikanth, T. V. Muni, M. VishnuVardhan, and D. Somesh, "Design and simulation of PV-wind hybrid energy system," *Journal of Advanced Research in Dynamical and Control Systems*, vol. 10, no. 4, pp. 999–1005, 2018.
- [11] T. V. Muni, G. S. S. Vidya, and N. R. Susan, "Dynamic modeling of hybrid power system with MPPT under fast varying of solar radiation," *International Journal of Applied Engineering Research*, vol. 12, no. 1, pp. 530–537, 2017.
- [12] K. S. Reddy, A. S. Priyanka, K. Dussarlapudi, and T. V. Muni, "Fuzzy logic based iUPQC for grid voltage regulation at critical load bus," *International Journal of Innovative Technology and Exploring Engineering*, vol. 8, no. 5, pp. 721–725, 2019.
- [13] S. Ilahi, M. S. Ramaiah, T. V. Muni, and K. G. Naidu, "Study the performance of solar PV array under partial shadow using DC-DC converter," *Journal of Advanced Research in Dynamical and Control Systems*, vol. 10, no. 4, pp. 1006–1014, 2018.
- [14] A. Elamathy, G. Vijayagowri, and V. Nivetha, "Bidirectional battery charger for PV using interleaved fourport DC-DC converter," *TELKOMNIKA Telecommunication, Computing, Electronics and Control*, vol. 14, no. 3, pp. 428–433, Jun. 2015, doi: 10.11591/telkomnika.v14i3.7894.
- [15] A. Kaviani-Arani and A. Gheiratmand, "Soft switching boost converter solution for increase the efficiency of solar energy systems," *TELKOMNIKA Telecommunication, Computing, Electronics and Control*, vol. 13, no. 3, pp. 449–457, Mar. 2015, doi: 10.11591/telkomnika.v13i3.7127.





- [16] A. T. M. and M. Prabhakar, "An efficient high gain dc-dc converter for automotive applications," *International Journal of Power Electronics and Drive Systems (IJPEDS)*, vol. 6, no. 2, pp. 242–252, Jun. 2015, doi: 10.11591/ijpeds.v6.i2.pp242-252.
- [17] Z. Zhang and K.-T. Chau, "Pulse-width-modulationbased electromagnetic interference mitigation of bidirectional grid-connected converters for electric vehicles," *IEEE Transactions on Smart Grid*, vol. 8, no. 6, pp. 2803–2812, Nov. 2017, doi: 10.1109/TSG.2016.2541163.
- [18] O. C. Onar, J. Kobayashi, D. C. Erb, and A. Khaligh, "A bidirectional high-power-quality grid interface with a novel bidirectional noninverted buck-boost converter for PHEVs," *IEEE Transactions on Vehicular Technology*, vol. 61, no. 5, pp. 2018–2032, Jun. 2012, doi: 10.1109/TVT.2012.2192459.
- [19] M. B. Camara, H. Gualous, F. Gustin, A. Berthon, and B. Dakyo, "DC/DC converter design for supercapacitor and battery power management in hybrid vehicle applications—Polynomial control strategy," *IEEE Transactions on Industrial Electronics*, vol. 57, no. 2, pp. 587–597, Feb. 2010, doi: 10.1109/TIE.2009.2025283.
- [20] T. Bhattacharya, V. S. Giri, K. Mathew, and L. Umanand, "Multiphase bidirectional flyback converter topology for hybrid electric vehicles," *IEEE Transactions on Industrial Electronics*, vol. 56, no. 1, pp. 78–84, Jan. 2009, doi: 10.1109/TIE.2008.2004661.
- [21] Z. Amjadi and S. S. Williamson, "A novel control technique for a switched-capacitor-converter-based hybrid electric vehicle energy storage system," *IEEE Transactions on Industrial Electronics*, vol. 57, no. 3, pp. 926–934, Mar. 2010, doi: 10.1109/TIE.2009.2032196.
- [22] F. Z. Peng, F. Zhang, and Z. Qian, "A magnetic-less DC-DC converter for dual voltage automotive systems," in *Conference Record of the 2002 IEEE Industry Applications Conference. 37th IAS Annual Meeting (Cat. No.02CH37344)*, 2002, vol. 2, pp. 1303–1310, doi: 10.1109/IAS.2002.1042726.
- [23] A. Nasiri, Z. Nie, S. B. Bekiarov, and A. Emadi, "An on-line UPS system with power factor correction and electric isolation using BIFRED converter," *IEEE Transactions on Industrial Electronics*, vol. 55, no. 2, pp. 722–730, 2008, doi: 10.1109/TIE.2007.911199.
- [24] B. P. Ganthia, R. Dharmaparakash, T. Choudhary, T. Vijay Muni, Essam A. Al-Ammar, A. H. Seikh, M. H. Siddique, A. Diriba, "Simulation Model of PV System Function in Stand-Alone Mode for Grid Blackout Area," *International Journal of Photoenergy*, vol. 2022, pp. 1-12, 2022, doi: 10.1155/2022/6202802.
- [25] V. A. Krishnan *et al.*, "An IOT Innovation of Smart Solar Energy Consumption Analysis and Control in Micro Grid", *International Journal of Photoenergy*, vol. 2022, pp. 1-8, 2022, doi: 10.1155/2022/7506237.

BIOGRAPHIES OF AUTHORS







Podila Purna Chandra Rao     completed B.Tech. and M.Tech. from JNT University, Andhra Pradesh. He is pursuing Ph.D. in Annamalai University. His area of interest is power electronic converters, electric vehicles. He can be contacted at email: purnachandrarao.phd@gmail.com.



Dr. Radhakrishnan Anandhakumar     is working as Assistant Professor in the Department of Electrical Engineering, Faculty of Engineering and Technology, Annamalai University, Annamalai Nagar, Tamilnadu, India. His area of interest includes optimization techniques in the power systems, and power system reliability. He can be contacted at email: anand_r1979@yahoo.com.



Dr. L. Shanmukha Rao     Research Co-Guide, Professor, Electrical and Electronics Engineering, Kallam Haranadhareddy Institute of Technology, Chowdavaram, Guntur, Andhra Pradesh, India. His area of interest includes FACTS devices, power quality, deregulated power systems, and renewable energy resources. He can be contacted at email: lsrlingineni@yahoo.co.in.